

A case of abdominal mesenteric Castleman's disease with left renal cell carcinoma and stomach leiomyoma

Shunjun Chen¹ MD,
Lele Song² MD,
Xinli Xie¹ MD, PhD,
Xingmin Han¹ MD,
Bing Cheng¹ MD, PhD

1. Department of Nuclear Medicine,
The First Affiliated Hospital of
Zhengzhou, University Zhengzhou
City, Henan Province, China, 450052

2. Department of CT Room,
The First Affiliated Hospital of
Henan, University of Science and
Technology, Luoyang City, Henan
Province, China, 471003

Keywords: -Castleman's disease
-Renal cell carcinoma
-Stomach leiomyoma

Corresponding author:

Bing Cheng MD
Department of Nuclear Medicine,
The First Affiliated Hospital of
Zhengzhou University,
Zhengzhou City, Henan Province,
China, 450052

Received:

2 September 2016

Accepted revised:

21 October 2016

Abstract

A rare case of abdominal mesenteric Castleman's disease with left renal cell carcinoma and stomach leiomyoma is reported. A 57 years old male patient was transferred to our hospital for investigation of a left kidney tumor. Physical examination and routine laboratory tests were normal. Multi mode imaging by 64-slices spiral computed tomography (CT) scan, the enhanced CT scan and the fluorine-18-fluorodeoxyglucose positron emission tomography/CT (¹⁸F-FDG PET/CT) scan were applied. Computed tomography showed a 5.4cm×5.2cm mass in the abdomen. The radioactive distribution of the mass was high SUVmax about 4.5. Furthermore, a soft tissue mass, about 3.9cm×3.0cm, was detected in the left kidney, with significantly inhomogeneous enhancement in the arterial phase of the CT scan, while contrast agent CT showed activity in the venous phase. The radioactive distribution of this mass was slightly concentrated and its SUVmax was about 3.2. With the stomach filled with water, an oval shaped and slightly lobulated soft tissue mass was also observed in the cardia, with a size about 4.6cm×3.0cm. Computed tomography showed mild enhancement of radioactively in the arterial phase and delayed enhancement in the venous phase. The radioactive distribution of the mass was diffused and SUVmax was about 4.7. **Conclusion:** The patient was operated and pathology showed: a) A mesenteric mass and abdominal lymph nodes with cells of the hyaline vascular type of Castleman's disease. b) Renal clear cells carcinoma of the left kidney and c) Spindle cells leiomyoma tumor in the gastric cardia. Three tumors in the same patient are extremely rare.

Hell J Nucl Med 2016; 19(3):285-288

Published online: 10 December 2016

Introduction

Castleman's disease (CD) is a rare atypical lymphatic tissue hyperplasia first reported in 195[1]. Castleman's disease can occur in any part of the lymphatic system and predilection sites are: mediastinum, neck, abdomen, pelvis armpit and other, while CD rarely occurs in the mesenteric area. Castleman's disease can affect multiple systems and is manifested or may be accompanied by nephrotic syndrome, membranous glomerulonephritis, edema or serous effusion, interstitial pneumonia, vasculitis, peripheral neuritis, myasthenia gravis, Sjogren's syndrome, amyloidosis, stomatitis or keratitis, endocrine gland dysfunction, skin diseases, autoimmune cytopenias, thrombotic thrombocytopenia, thrombocytopenic purpura, bone marrow fibrosis, polyneuropathy, organomegaly, endocrinopathy, skin changes and other. In this report, the multi mode imaging by tomography/CT (¹⁸F-FDG PET/CT) image supported the diagnosis of abdominal mesenteric Castleman's disease, left renal clear cells carcinoma and gastric leiomyoma.

Case Report

A 57 years old male patient was transferred to our hospital for investigation of a left kidney tumor. The tumor was incidentally found by a routine abdominal ultrasound examination in a local hospital. He had no significant medical or surgical history. Physical examination and routine laboratory tests were normal. Computed tomography showed a 5.4cm×5.2cm mass in the abdomen, CT value about was 44Hu. The mass, was homogeneous isodense with irregular or lobular margins located in the intraperitoneal area, adjacent to the mesenteric root. Computed tomography also showed significantly homogeneous enhancement in the arterial phase with CT value of about 179Hu. Contrast

agent CT showed in the venous phase slightly decreased value of about 121Hu. Furthermore, Computed Tomography Angiography (CTA) showed that there were tortuous and thick nutrient arteries around the mass originated from the superior mesenteric arteries draining to the superior mesenteric veins. The radioactive concentration of the mass was increased, and SUVmax was about 4.5. Multiple lymph nodes were observed around the mass. The size of the larger lymph nodes was about 1.3cm×1.1cm.

Furthermore a soft tissue mass was observed in the left kidney, with less clear boundaries, inhomogeneous density and size about 3.9cm×3.0cm. Computed tomography showed significantly inhomogeneous enhancement in the arterial phase, while contrast agent CT showed decreased venous phase. Computed Tomography Angiography showed that there were small branches of renal artery feeding the mass. The radioactive distribution was slightly concentrated in the mass and the SUVmax was about 3.2.

In the filled by water stomach, an oval shaped and slightly lobulated soft tissue mass, with size of about 3.0cm×4.6cm was observed in the cardia, with homogeneous inner density CT value about 40Hu, mild CT enhancement in the arterial phase with CT value about 49Hu, and delayed enhancement in the venous phase with CT value about 61Hu. The radioactive distribution of the mass was diffuse and SUVmax was about 4.7.

Abdominal mass resection, laparoscopic left renal radical resection and proximal stomach resection were performed. The lesion in the left kidney was considered as renal clear cells carcinoma. The mesenteric mass abdominal lymph nodes was diagnosed as Castleman's disease of the hyaline vascular type and the lesion in the gastric cardia as gastric spindle cells leiomyoma.

In the follow-up after 3 months, no recurrences or metastases were diagnosed.

Discussion

Castleman's disease is a chronic lymphatic tissue hyperplasia with atypical clinical features, characterized by non-neoplastic lymph nodes enlargement, also known as giant lymph node hyperplasia or vascular lymphoid follicular hyperplasia. At present, the pathogenesis of CD is not clear, and it may be associated with virus such as human herpes virus-8, HHV-8 infection, abnormal regulation of cytokines (such as interleukin-6, IL-6), angiogenesis and other [2-4]. Computerized tomography can be classified into unicentric Castleman's disease (UCD) and multicentric Castleman's disease (MCD) according histologic and clinical characteristics. There are three histologic types of CD that have been described: a) Hyaline-vascular CD (HV-CD) usually asymptomatic with lymph nodes enhancement, and benign clinical course. b) Plasma cells CD (PC-CD) which often has multiple lesions and may be accompanied by fever, emaciation, anemia, skin rash which hypergammaglobulinemia and other systemic symptoms. c) Mixed CD (M-CD) which has symp-

toms similar to that of PC-CD [3]. Hyaline-vascular CD (HV-CD) which represents 90% of CD cases and is usually unicentric [3-5]. This type most commonly occurs in UCD. The CT of UCD more often shows a shadow of a mass with clear boundaries, of round or lobulated shape and uniform density [6]. Calcifications are rare. Punctuated and branching calcifications can be seen in some of these masses, and are caused by the hyalinization and degeneration of vessels [7]. The masses are rarely accompanied by hemorrhagic and necrotic foci, which may be related to abundant blood supply or good collateral circulation. The whole body imaging by ¹⁸F-FDG PET/CT in CD mainly reveals celiac lymph nodes with lesions with slightly increased metabolism closer to SUVmax 5.8±4.1(2.4-17.1) as reported by Lee et al. (2013) and others [8]. It must be noted that some atypical lesions show higher uptake with increased SUV delayed images, which may be related to the degree of the disease progression, suggesting that the disease may develop into lymphoma. The above authors suggested that if MCD shows high FDG uptake, the prognosis is poor. Their patient also suffered from renal clear cell carcinoma, which is one of the most common malignant tumors of the urinary system. The preferred method for the diagnosis of renal cell carcinoma, with high detection rate is CT which is able to show the size, shape, tissue density, edge condition, internal structure and invasion extent to the adjacent tissues and organs and also to show blood supply of the mass through enhancement. The detection of recurrence and metastases did not interfere with urinary excretion. Sensitivity and specificity reached 60%-88% and 75%-100% respectively. Retroperitoneal lymph nodes were detected [9, 10].

Our patient also had gastric cardia leiomyoma. Gastric benign tumors account for a small number of gastric tumors while gastric cardia leiomyoma is the most common type of gastric benign tumors. Gastric leiomyoma often occurs in the fundus of the stomach, stomach body, and antrum. The CT findings include: a) Most of the lesions are <5cm, smooth or slightly lobulated, with clear boundaries b) The lesions show homogeneous or inhomogeneous progressive uptake. The delayed phase shows more significant uptake among the three-phase scan, while the peak time of uptake is longer than that of the gastric cancer. c) Enhanced uptake lesions are adjacent to gastric wall, grow with or without adjacent structure constrictions, and have no obvious infiltration signs.

Conclusions

In conclusion, we reported a rare case of synchronous Castleman's disease with left renal cell carcinoma and gastric cardia leiomyoma. The ¹⁸F-FDG uptake of gastric leiomyoma was similar to that of the soft tissues in the mesenteric area, therefore was easy to be misdiagnosed. However, the extent and mode of CT dynamic enhancement supported diagnosis. The imaging manifestations of the lesions were different, in accordance with the relevant literature reports.

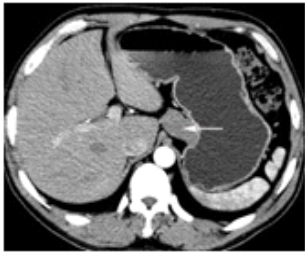


Figure 1.

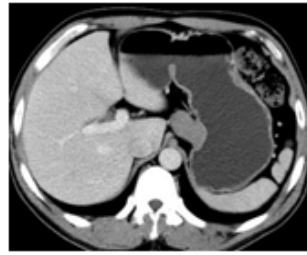


Figure 2.

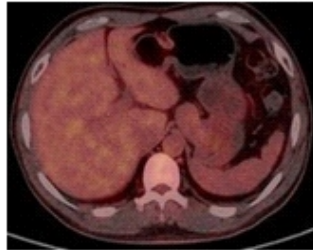


Figure 3.

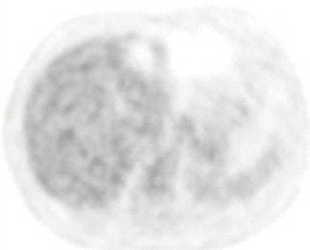


Figure 4.

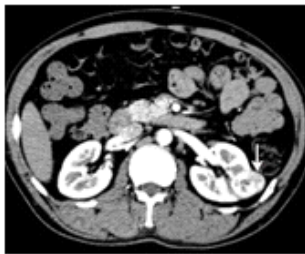


Figure 5.



Figure 6.

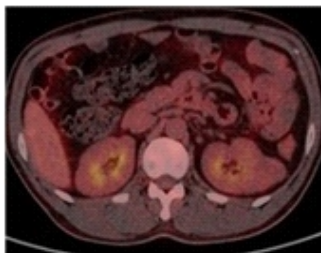


Figure 7.

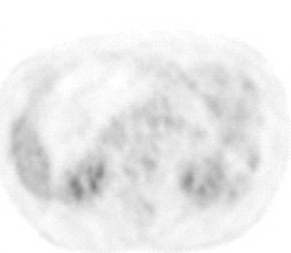


Figure 8.



Figure 9.



Figure 10.



Figure 11.

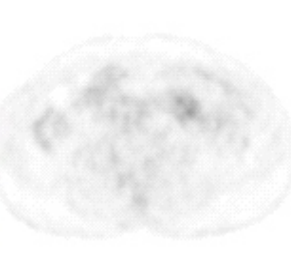


Figure 12.

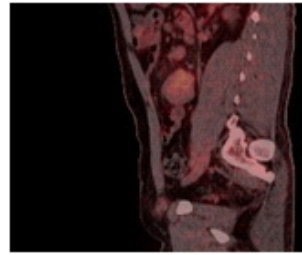


Figure 13.

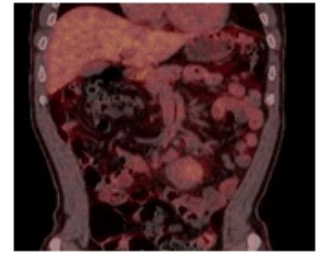


Figure 14.



Figure 15.

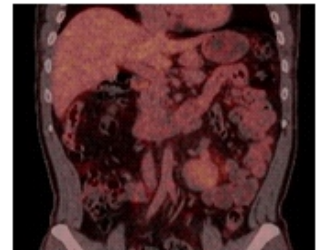


Figure 16.

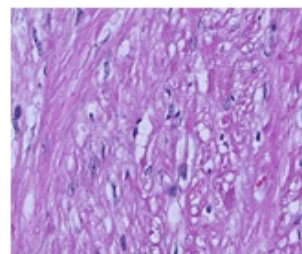


Figure 17.

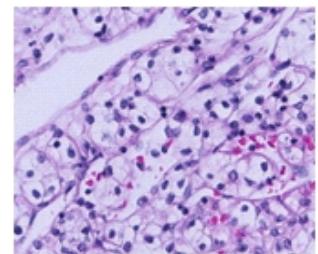


Figure 18.

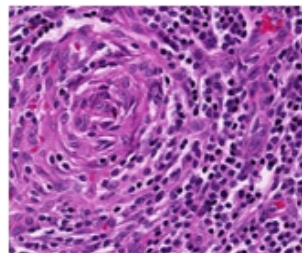


Figure 19.

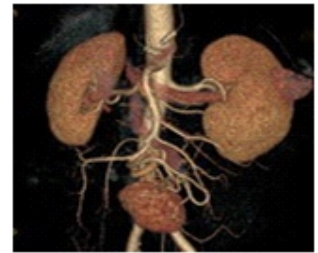


Figure 20.

Figures 1-20 are: 64 slice CT arterial phase, venous phase, PET/CT fusion and PET imaging. The lesions in gastric cardia (arrow) showed homogeneous and mild enhancement in the arterial phase delayed enhancement in the venous phase, and SUVmax 4.7 indicating active metabolism. Figures 5-8 are: 64-slice CT arterial phase, venous phase, PET/CT fusion and PET images which showed: space occupying lesions in the left kidney (arrow) inhomogeneous enhancement in the arterial phase decreased uptake in Venous phase, and SUVmax 3.2. Figures 9-12 and Figure 20 showed lesions in the left abdominal cavity (arrow) with clear boundaries and slightly lobulated shape, with homogeneous uptake in the arterial phase and contrast agent slightly decreased in the venous phase, like that of the aorta. Tortuous and thick nutrient artery originated from the superior mesenteric artery and superior mesenteric vein. Veins can be seen around the lesions. The extent of uptake was active and the SUVmax was about 4.7. Figures 13, 11, 14, 15, 16 showed PET/CT fusion

images showed left abdominal lesions at the axial view, sagittal view and the coronal view, respectively. Figures 17-19 showed pathological sections of the gastric cardia leiomyoma, renal clear cell carcinoma and celiac mesenteric Castleman's disease (transparent vascular type), respectively shown in the light microscope 400, HE stain. Figure 20 showed CTA the shape, of the feeding artery and of the draining vein of CD.

Bibliography

1. Castleman B, Iverson L, Menendez VP. Localized mediastinal lymphnode hyperplasia resembling thymoma *Cancer* 1956; 9(4): 822-30.
2. Farruggia P, Trizzino A, Scibetta N, et al. Castleman's disease in childhood: report of three cases and review of the literature. *Ital J Pediatr* 2011; 37: 50.
3. Bonekamp D, Horton KM, Hruban RH, Fishman EK. Castleman disease: the great mimic. *Radiographics : Radiographics* 2011; 31: 1793-807.
4. Ramsay AD. Reactive lymph nodes in pediatric practice. *Am J Clin Pathol* 2004; 122: S87-S97.
5. Lin CY, Chang YL. Castleman's disease in the head and neck region: meta-analysis of reported cases in Taiwan and literature review. *J Formos Med Assoc* 2010; 109: 913-20.
6. Nishie A, Yoshimitsu K, Irie H et al. Radiologic features of Castleman's disease occupying the renal sinus. *AJR* 2003; 181(4): 1037-40.
7. Wang RG, Na J, Bin HY et al. Characteristic calcification of localized Castleman's disease: CT and histopathologic appearance[J]. *Chin J Radiol* 2002; 36(4): 354-56.
8. Lee ES, Paeng JC, Park CM et al. Metabolic characteristics of Castleman disease on ¹⁸F-FDG PET in relation to clinical implication. *Clin Nucl Med* 2013; 38(5): 339-42.
9. Ak I, Can C. F-18 FDG PET in detecting renal cell carcinoma. *Acta radiologica* 2005; 46(8): 895-9.
10. Kang DE, White RL, Jr., Zuger JH et al. Clinical use of fluorodeoxyglucose F-18 positron emission tomography for detection of renal cell carcinoma. *J Urol* 2004; 171(5): 1806-9.